

See discussions, stats, and author profiles for this publication at: <https://www.researchgate.net/publication/274084883>

An Unusual Electrochemical Reductive Cleavage of Azo Dye into Highly Redox Active Copolymeric Aniline Derivatives on a MWCNT Modified Electrode Surface at Neutral pH and Its Electr...

ARTICLE *in* THE JOURNAL OF PHYSICAL CHEMISTRY C · MARCH 2015

Impact Factor: 4.77 · DOI: 10.1021/acs.jpcc.5b00612

READS

71

3 AUTHORS:



Gayathri Prakasam

VIT University

8 PUBLICATIONS 73 CITATIONS

[SEE PROFILE](#)



Annamalai Senthil Kumar

VIT University

129 PUBLICATIONS 2,175 CITATIONS

[SEE PROFILE](#)



Sriraghavan Kamaraj

VIT University

54 PUBLICATIONS 398 CITATIONS

[SEE PROFILE](#)

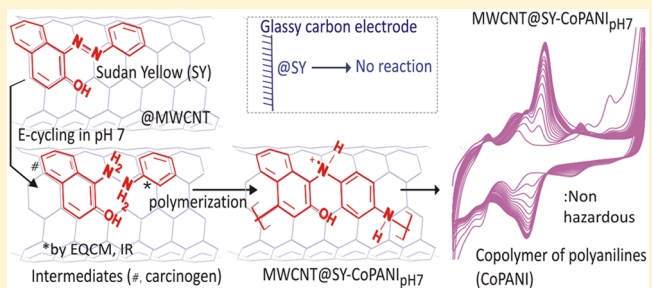
An Unusual Electrochemical Reductive Cleavage of Azo Dye into Highly Redox Active Copolymeric Aniline Derivatives on a MWCNT Modified Electrode Surface at Neutral pH and Its Electroanalytical Features

Prakasam Gayathri,[†] Annamalai Senthil Kumar,^{*,†} and Sriraghavan Kamaraj[‡]

[†]Environmental and Analytical Chemistry Division, and [‡]Organic Chemistry Division, School of Advanced Sciences, Vellore Institute of Technology University, Vellore-632 014, India

Supporting Information

ABSTRACT: Developments of new decomposition or degradation methods of environmentally hazardous azo dyes from textile industries are very important. Usually, strong acid-based chemical/electrochemical and neutral pH-based bacterial decomposition methods were widely used. Here, we report a mild, simple, and facile electrochemical method for decomposition of azo dye (Sudan yellow; SY) into a highly redox active copolymer of polyanilines via aniline derivatives as intermediates on a MWCNT modified glassy carbon electrode (GCE/MWCNT) surface unusually in a neutral pH using phosphate buffer solution (PBS) (GCE/MWCNT@SY-CoPANI_{pH7}). One of the intermediate products, aniline ($M_w = 93 \text{ mol g}^{-1}$, calculated) was identified by an in situ cyclic voltammetry-electrochemical quartz crystal balance experiment. No such SY electrochemical reaction was observed on a naked GCE surface. Physico-chemical characterizations by TEM, Raman, IR, and UV-vis spectroscopic methods supported the formation of polymeric product on MWCNT surface (GCE/MWCNT@SY-CoPANI_{pH7}). Electroanalytical performance of this new electrode was tested using ascorbic acid (AA) and Fe(CN)₆³⁻ as models. Interestingly, a dilute solution of Nafion (Nf) casted modified electrode system (GCE/MWCNT@SY-CoPANI_{pH7}/Nf) showed improved electroanalytical performance, unlike the conventional Nafion modified system (GCE/MWCNT/Nf) with vanished peak current response due to the electrostatic repulsive interaction between the anionic AA ($pK_a = 4.10$), Fe(CN)₆³⁻ ion, and anionic sulfonic acid groups in Nafion. A zwitter ionic complex between a polaronic copolyaniline and sulfonic acid of Nafion is proposed as a possible structure for the newly developed hybrid system. Using the GCE/MWCNT@SY-CoPANI_{pH7}/Nf, a selective flow injection analysis of AA has been demonstrated as an analytical application with good recovery values.



1. INTRODUCTION

The development of new functional electrodes having stable and highly redox electrochemical characteristics and the ability to mediate oxidation/reduction of specific analyte is a continued research interest in electroanalytical chemistry. Azo dyes are synthetic aromatic compounds with one or more $-N=N-$ bonds. Because of their specific physicochemical and biological properties, azo dyes exhibit broad applications in pharmaceutical (antibiotic, antimicrobial, antifungal, and anti-HIV activities), medical, cosmetic, food, dyeing/textile industry, and analytical chemistry.¹ However, the most typical and popular field of utility remains their coloring function. Around 10 000 of these compounds are described, and more than 2000 are applied to color various materials.^{1,2} As compared to natural dyes, the synthetic azo dyes have many qualities such as high stability to light, oxygen, and pH, low microbiological adulteration, and color consistency.¹ Research has shown that some azo dyes pose very serious health risks (like carcinogenic) to humans if they are used in particular textiles and if they

percolate into certain water supplies.^{3,4} In fact, these azo dyes are metabolized to the corresponding carcinogenic amine derivatives by liver enzymes in animals and humans.^{5,6} In 2002, the European Union responded by banning azo dyes that could break down into carcinogenic amine products.^{7,8} Thus, a simple method for the cleavage or decomposition of azo dyes is an important research interest in environmental chemistry. So far, harsh chemical (reagents such as KMnO₄, K₂Cr₂O₇, Fenton, and H₂O₂ coupled UV-vis were used),^{9–11} photochemical,^{10,12} and electrochemical (assisted via a Cl₂/Cl⁻ redox couple or electron-Fenton) methods were used for the decomposition of the azo dyes.^{13,14} The drawbacks of the above-reported methods are high operating costs, slower reaction rates, strong acidic medium, and they also involve destructive techniques. However, anaerobic bacteria such as *Eubacterium hadrum*,

Received: January 21, 2015

Revised: March 15, 2015

Clostridium clostridiiforme, *Butyrivibrio* sp., *Bacteroides* sp., *Clostridium paraputreficum*, and *Clostridium nexile* have been utilized for the selective reduction of azo dyes to aniline derivatives that are potentially well-known carcinogenic agents, in a neutral pH.^{15,16} Herein, we report a simple electrochemical decomposition/decolorization of azo dye to a highly redox active copolymer of polyanilines, via aniline derivatives, on a multiwalled carbon nanotube (MWCNT) modified glassy carbon electrode (GCE/MWCNT) surface interestingly in a neutral pH solution.

Carbon nanotubes (CNTs) have remained in the forefront of intense research for more than a decade, due to their exceptional physical, chemical, and electronic properties that have been inherited from the parent in-plane graphite.¹⁷ A notable characteristic of CNT is their interaction with other molecules.^{18,19} CNTs have been used as an efficient adsorbent for the removal of the azo dyes from the wastewater.²⁰ Azo dye adsorbed TiO₂ immobilized-CNTs have been found to be potential photochemical systems for the decolorization.²¹ The strong $\pi-\pi$ interaction between the graphitic sp² carbons in CNT and the aromatic sp² in the azo dyes favors the aforesaid applications.²² Meanwhile, Genies et al. reported electro-oxidation of azobenzene to aniline product and further to electro-polymerization as polyaniline on a platinum electrode surface at 1.4 V vs Cu/CuF₂ in NH₄F+HF solution under acidic medium.²³ It is well-known that HF is a highly dangerous gas and can even cause death if high concentration is exposed to human. Generally, it is highly challenging to electro-oxidize the azo bond and electropolymerize the aniline to polyaniline in a neutral condition. Herein, we observe a facile electrochemical conversion of azo dye to a copolymer of polyaniline, via aniline derivatives as intermediates, on a multiwalled carbon nanotube (MWCNT) modified electrode surface in a neutral pH solution, which mimics the anaerobic bacterial reduction of azo dyes to aniline derivatives. This new chemically modified electrode shows an excellent electroanalytical activity to Vitamin C (ascorbic acid, AA) and has several advantages over the conventional electrochemical methods such as (i) simple method for electrochemical decomposition of azo dye unusually in a neutral pH, (ii) low potential cleavage of azo bond and in situ polymerization of carcinogenic aniline derivatives as a nonhazardous copolymer of polyanilines on a low cost impure-MWCNT surface, and (iii) recycling of azo dye waste into highly useful redox active polyaniline systems.

2. EXPERIMENTAL SECTION

2.1. Chemicals and Reagents. Sudan yellow, Sudan red, methyl red, MWCNTs (>90% carbon basis, outer diameter, 10–15 nm; inner diameter, 2–6 nm; length, 0.1–10 μ m), single walled carbon nanotube (SWCNTs; 50–70% carbon basis, outer diameter is 1–1.5 nm), and 5% Nafion dissolved in lower aliphatic alcohols were purchased from Sigma-Aldrich. Other chemicals used were all of ACS-certified reagent grade and used without further purification. Aqueous solutions were prepared using deionized and alkaline potassium permanganate distilled water. The supporting electrolyte, pH 7 phosphate buffer solution (PBS) of ionic strength, $I = 0.1 \text{ mol L}^{-1}$, was used throughout this work.

2.2. Instrumentation. Voltammetric measurements were carried out with a CHI model 660C electrochemical workstation (U.S.). The three-electrode system consists of GCE and its chemically modified electrodes (CMEs) as a working electrode (0.0707 cm^2), Ag/AgCl as a reference, and platinum

wire as the auxiliary electrode. The bioanalytical system (BAS, U.S.) polishing kit was used to polish the GCE surface. In situ CV-EQCM experiments were carried out using a gold single crystal electrode (EQCM-Au) of geometric surface area = 0.19 cm^2 with a CHI 440 B workstation (U.S.). The flow injection analysis (FIA) system is comprised of a Hitachi L-2130 pump delivery (Japan), a Rehodyne model 7125 sample injection valve (20 mL loop) with interconnecting Teflon tube, and a conventional electrochemical detector system (BAS, U.S.). FTIR analysis was carried out using a JASCO 4100 spectrophotometer by KBr method. A V-670 spectrometer (JASCO, Japan) was used for the UV-vis measurements. Raman spectroscopic analysis was carried out using AZILTRON, PRO 532 (USA) with a 532 nm laser excitation source. For transmission electron microscopic (TEM) examination of MWCNT and its modified systems, a JEOL JEM 2100 machine was used.

2.3. Electrochemical Studies with MWCNT Modified Electrode. Purified MWCNT (p-MWCNT, p = purified) and functionalized MWCNT (f-MWCNT, f = functionalized) samples were prepared by heating pristine MWCNT (200 mg) in 35 mL of 6 M (for p-MWCNT) or 15 M HNO₃ (for f-MWCNT) in a silicone oil bath at reflux for 12 h ($T = 413 \text{ K}$). The product was filtered and washed with copious amounts of distilled H₂O until the pH of the filtrate solution become neutral, and the samples were dried at $T = 350 \text{ K}$ in a vacuum oven. Physico-chemical characterizations of the impure MWCNT and f-MWCNT samples by thermogravimetric analysis (TGA) and powder X-ray diffraction (XRD) showed the presence of 6.88% and 2.20% impurities, respectively, due to metal oxides (Fe₂O₃, NiO, and Co₂O₃), graphitic traces, and amorphous carbon.²⁴

Prior to the modification, the surface of the GCE was cleaned both mechanically (polished with 1 μ alumina powder in the BAS polishing kit, cleaned with acetone, followed by DD water) and electrochemically (by performing cyclic voltammetry (CV) for 10 cycles in the potential window from -0.2 to 1 V vs Ag/AgCl in pH 7 PBS at scan rate (v) 50 mV s⁻¹). GCE/CNT modified electrode was prepared by drop casting of 5 μL of an aliquot from 1 mg of CNT dispersed in 500 μL of ethanol, 10 min sonication of the stock solution on a cleaned GCE electrode, and drying the electrode in air for 2 min at room temperature followed by drop casting of 5 μL of 2 mg of azo dye dissolved in 500 μL of ethanol solution on the surface of GCE/CNT. Prior to the electrochemical studies, the GCE/CNT@SY modified electrode was electrochemically pretreated in a potential window from -0.5 to 0.5 V vs Ag/AgCl in pH 7 PBS at a $v = 50 \text{ mV s}^{-1}$ (no. of cycles (n) = 30).

2.4. Real Sample Analyses. Grape juice (#1), pharmaceutical tablet (#2), and three different supplementary food products (as tablets, #3–#5) were purchased from a local supermarket and medical center. These samples were stored in the refrigerator until use. Prior to the FIA, the fruit juice was filtered using a syringe filter (Nupore, 0.22 μm) and suitably diluted with pH 7 PBS. The tablet samples were crushed into powders and then suitably dissolved in pH 7 PBS. The standard addition method was adopted for real sample analysis.

3. RESULTS AND DISCUSSION

3.1. Electrochemistry of Azo Dye on MWCNT Surface. Initially, Sudan yellow (SY) was taken as a model compound to study the electrochemical behavior of azo dye on MWCNT surface. Figure 1A shows 20 continuous CV responses of dilute

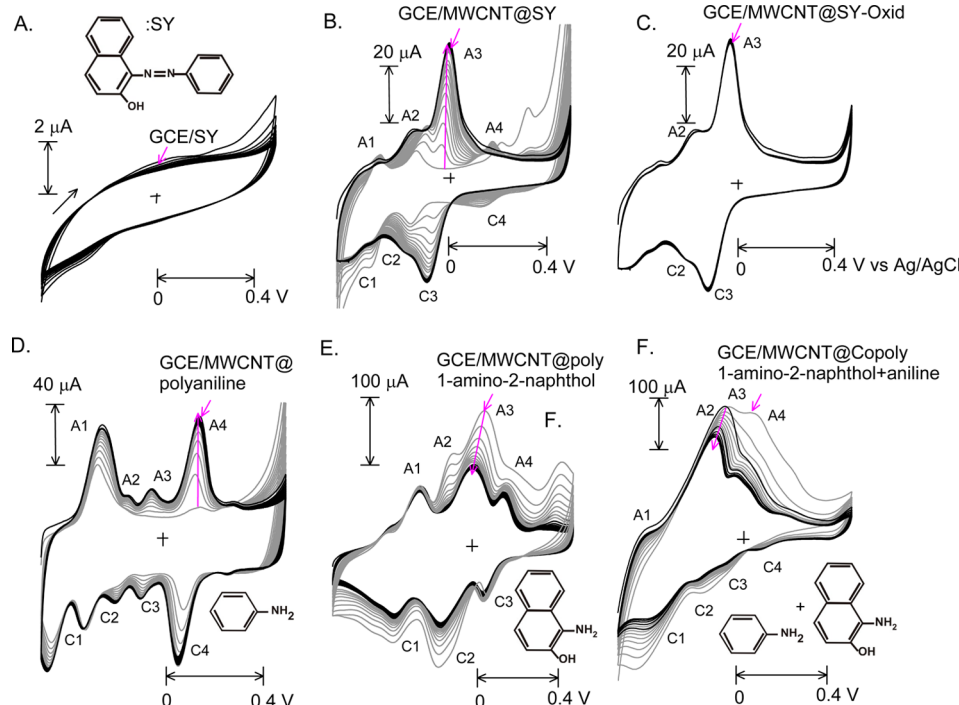


Figure 1. Twenty continuous CV responses of Sudan yellow dye (SY) adsorbed GCE (A) and GCE/MWCNT (B), and aniline (D), 1-amino-2-naphthol (E), and a mixture of aniline and 1-amino-2-naphthol adsorbed GCE/MWCNTs in a pH 7 phosphate buffer solution at a scan rate of 50 mV s^{-1} . Part (C) is the 20 CV of GCE/MWCNT@SY-Oxid system. Note: SY-Oxid = SY-CoPANI_{Ph7}. Insets are the chemical structures of the respective compounds.

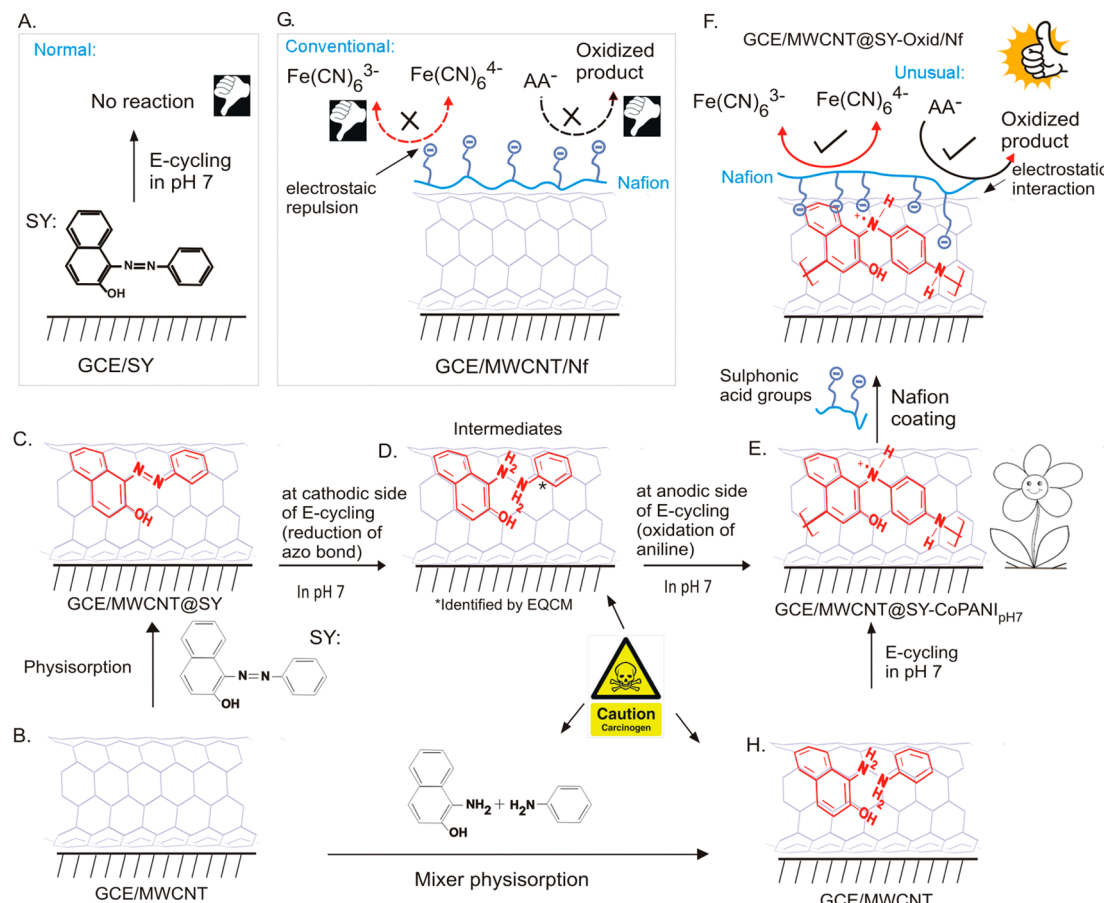
SY-ethanol solution drop-casted GCE in a potential window from -0.5 to $+0.5$ V vs Ag/AgCl in pH 7 PBS at $v = 50 \text{ mV s}^{-1}$. No faradic response was observed with the above GCE modified system indicating electro-inactivity of the SY on the conventional electrode in a neutral pH solution (Scheme 1A). Interestingly, when the above experiment was repeated on a GCE/MWCNT surface, a feeble oxidation peak at 0.4 V vs Ag/AgCl in the first cycle and the appearance of several well-defined redox peaks at equilibrium potentials ($E_{1/2}$) of -0.3 (A1/C1), -0.18 (A2/C2), -0.02 (A3/C3), and 0.15 V vs Ag/AgCl (A4/C4), wherein the A3/C3 peak showed the maximum peak current signal, in subsequent CV cycles were noticed (Figure 1B, Scheme 1B and C). Thirty continuous E-cyclings of the modified electrode in a blank pH 7 PBS did not show any marked alteration in the redox peak, highlighting good stability of the system (Figure 1C). The calculated relative standard deviation (RSD) value for the A3 peak is 1.6% ($n = 10$ cycles). These results confirm selective electrochemical reaction of the azo dye on the GCE/MWCNT electrode surface in neutral pH solution. The above chemically modified electrode is designated as GCE/MWCNT@SY-Oxid, where the SY-Oxid = SY oxidized species. It is expected that intermediate products like aniline and 1-amino-2-naphthol might be formed during the cathodic side (Scheme 1D) and these intermediates might subsequently be oxidized into polyaniline derivative upon the anodic part of CV of the GCE/MWCNT@SY (Scheme 1E).

Next, the effect of applied potential on the cleavage of SY's azo bond and subsequent electro-polymerization reaction on GCE/MWCNT surface was examined (Supporting Information Figure S1). In the first set of E-cycling experiments, the starting potential of the working electrode (GCE/MWCNT) was kept constant at -0.7 V, and the sweeping potentials were varied as 0.3 , 0.5 , 0.7 , 0.8 , and 1.0 V vs Ag/AgCl. Similarly, in

the second set of experiments, the starting positive potential was fixed at 0.4 V, and the end potentials were varied as -0.2 , -0.3 , -0.4 , -0.5 , and -0.7 V vs Ag/AgCl. In the first set, qualitatively similar but varied quantitative peak currents, whereas in the second set, a potential-dependent formation of the redox behaviors, in which the absence and presence of the A3/C3 peak at sweeping potentials, -0.2 to -0.3 V and $E > -0.4$ V, respectively, were noticed. These observations indicate a reductive cleavage of the azo bond possibly to aniline and 1-amino-2-naphthol as intermediates at -0.4 V vs Ag/AgCl (cathodic side) and subsequently electro-oxidation of these intermediate species to the highly redox active polymers at $+0.3$ V vs Ag/AgCl (anodic side).

To understand the details about the polymerization reaction, control electrochemical experiments were carried out with aniline, 1-amino-2-naphthol, and a 1:20 mixture of both compounds discretely on a GCE/MWCNT in pH 7 PBS (Figure 1, curves D–F, Scheme 1H). In the case of aniline polymerization, two well-defined redox peaks at potentials -0.25 and 0.15 V and two minor peaks at -0.05 and -0.13 V vs Ag/AgCl, where as with the 1-aminonaphthol polymerization, a major redox peak at 0.035 V and two minor peaks at -0.2 and 0.15 V vs Ag/AgCl, were observed. Comparison of the CV redox peaks of the above individual polymers with the redox peaks of MWCNT@SY-Oxid showed a similarity in the peak potentials but with a distinct variation in the peak currents. The similarities in the peak potentials suggest the electrochemical oxidation of SY on MWCNT surface is a copolymer of polyaniline and poly(1-amino-2-naphthol). In the case of a mixture of aniline and 1-amino-2-naphthol (1:20), a high background current signal along with overlapped redox peak response was observed that indicates the copolymerization between aniline and 1-amino-2-naphthol (Scheme 1H). Overall,

Scheme 1. Cartoon for the Sudan Yellow (SY) Adsorbed MWCNT Modified GCE Electrode (B and C) for the Electrochemical Conversion of SY to a Copolymer of Polyaniline and Poly-1-amino-2-naphthol (E) via Intermediates of Aniline Derivatives (D) on a MWCNT Surface and Its Nafion Modified System for Unique Electroanalytical Reactions of Ascorbic Acid and Ferricyanide Ions (F)^a



^a(A), (G), and (H) are control electrochemical reactions.

the in situ generation of aniline and 1-amino-2-naphthol from SY on MWCNT surface and subsequent copolymerization observed in this work is quite unique and superior to the conventional copolymerization on the MWCNT surface for generation of highly redox active peaks.

To identify the structure of intermediate(s) formed on the electrochemical reaction of SY on the MWCNT surface, an in situ CV-EQCM experiment with a SY adsorbed MWCNT modified Au-EQCM in pH 7 PBS was carried out. Molecular mass (M_w) of the electro-active species involved in the electrochemical oxidation/reduction can be calculated using the following formula: $M_w = F \times m/Q$, where, Q is the charge passed, M_w is the molar mass per electron (g mol^{-1} = molecular weight), and F is Faraday's constant.^{25,26} We have also successfully utilized this technique as an important characterization tool for the identification of intermediates such as hydroquinone,²⁶ quinoline-quinone,²⁷ and several oxygenated species on the electro-oxidation of phenol, quinoniline, and poly aromatic hydrocarbons such as anthracene²⁸ and pyrene,²⁹ respectively, at MWCNT modified Au-EQCM surface. A solid state in situ CV-EQCM response of an Au-EQCM/MWCNT@SY in pH 7 PBS at $v = 50 \text{ mV s}^{-1}$ is displayed in Figure 2A (Figure 2E, step a). As can be seen, the CV response of the Au-EQCM/MWCNT@SY-Oxid closely matches the GCE/MWCNT@SY-Oxid (Figure 1C). Following Saubery's equa-

tion, conversion of frequency (f) to weight change (Δm) was done using inbuilt software with the CHI 440B instrument. In the EQCM, when the potential swept from -0.5 to -0.2 V , a significant decrement in the Δm values, and at $E > 0.3 \text{ V}$, an exponential increment in the response, were noticed. This observation is parallel with the CV redox peak current responses of the GCE/MWCNT@SY, where current decrement at extreme potentials and increment at middle of the potential window, against increasing the cycle numbers, were noticed (Figure 1B). It is suspected that solubility of the SY's intermediates (aniline and 1-aminonaphthol), aniline is freely soluble and 1-aminonaphthol is insoluble in water, and collisions of the intermediate radicals have some control over the copolymer product formation (Figure 2E, step c). If aniline is formed as an intermediate in the CV preparation, then, due to its solubility, it might be diffused out from the MWCNT-solid surface to solution phase and would be subsequently oxidized into polymeric unit (diffusion controlled process) on MWCNT. In the case of 1-amino-2-naphthol intermediate, due to its insolubility nature, it could not be diffused out from the MWCNT surface, and hence it might be led to decreased peak current responses in the CV preparation. Interestingly, the stripped aniline intermediate, at a molecular weight of $92.5 \pm 1 \text{ g mol}^{-1}$, was identified by in situ EQCM in this work. Figure 2D is a plot of Δm (from EQCM) versus Δq (from CV) for the

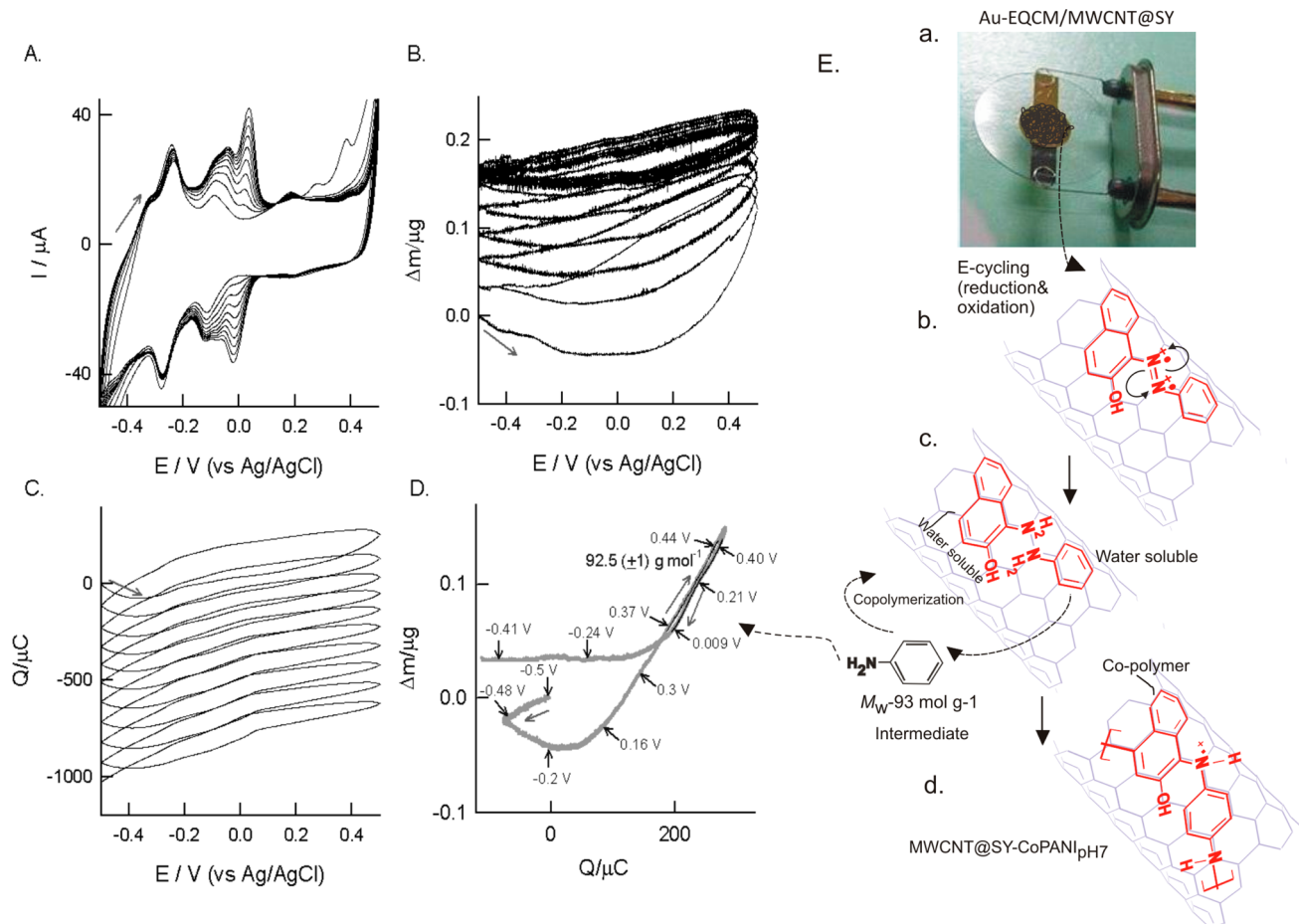


Figure 2. (A) In situ CV and EQCM responses of Au-EQCM/MWCNT@SY modified electrode in pH 7 PBS at $\nu = 50 \text{ mV s}^{-1}$. (B)–(D) are plots of Δm vs E/V vs Ag/AgCl , Q vs E/V vs Ag/AgCl , and Δm vs Q (first cycle), respectively. (E) is a cartoon for Au-EQCM/MWCNT@SY and its electrochemical mechanism for formation of copolymer of polyaniline and poly(1-amino-2-naphthol) via aniline and 1-amino-2-naphthol intermediates' electro-oxidation.

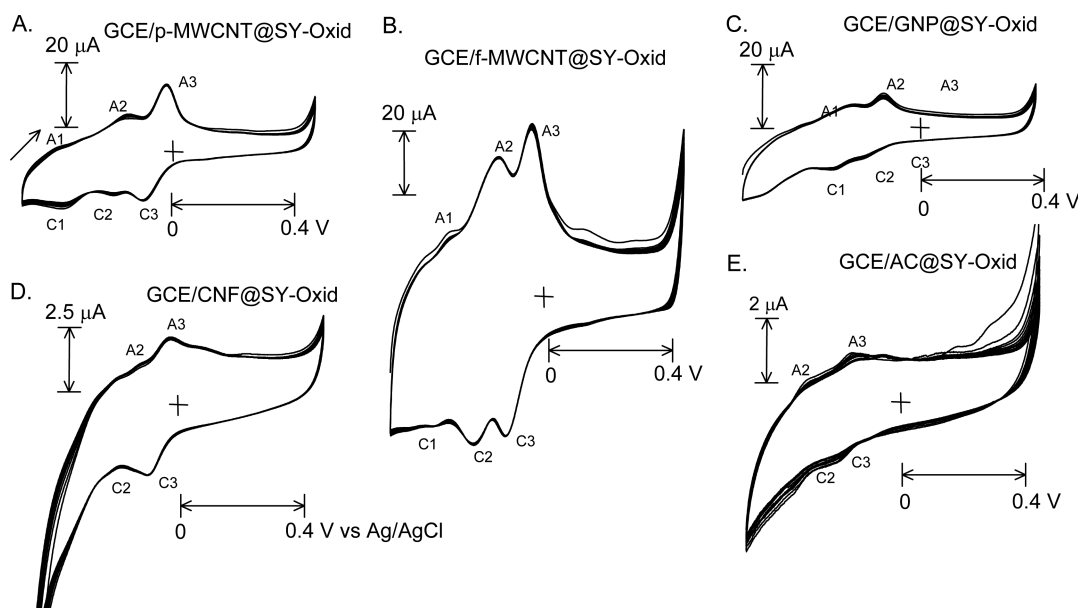


Figure 3. CV responses of (A) GCE/p-MWCNT@SY-Oxid, (B) GCE/f-MWCNT@SY-Oxid, (C) GCE/GNP@SY-Oxid, (D) GCE/CNF@SY-Oxid, and (E) GCE/AC@SY-Oxid in pH 7 PBS at a scan rate of 50 mV s⁻¹.

first cycle in situ CV-EQCM of Au-EQCM/MWCNT@SY. Significant weight loss (Δm) from -0.5 to -0.2 V vs Ag/AgCl

and exponential mass gain from 0.15 to 0.4 V in the forward anodic cycle of the CV experiment were noticed. From the

slopes of the forward and reverse regions, 0.37 to -0.44 V, a molecular mass, M_w , value 92.5 ± 1 g mol $^{-1}$, which corresponds to aniline ($M_w = 93.13$ g mol $^{-1}$), was calculated. The above result affirmed that SY-Oxid is a copolymer type of polyaniline and poly(1-amino-2-naphthol) (Figure 2E, step d). Hereafter, the GCE/MWCNT@SY-oxid is redesignated as GCE/MWCNT@SY-CoPANI_{pH7}, where SY-CoPANI_{pH7} = copolymer of polyaniline and poly(1-amino-2-naphthol) prepared from SY in pH 7 PBS.

In continuation to impure-MWCNT, other forms of carbons like purified-MWCNT, functionalized-MWCNT, graphite nanopowder (GNP), graphitized carbon nanofibre (CNF) and activated charcoal (AC) were also subjected to the SY electrochemical reaction in pH 7 PBS (Figure 3A–E). Except in the f-MWCNT case, which showed large background current with a couple of predominant peaks (A2 and A3), other carbon systems displayed qualitatively similar redox responses. With respect to the background corrected A3 peak current, the relative order of copolymerization on the carbon surface is impure-MWCNT (100%) > functionalized-MWCNT (90%), purified-MWCNT (59%), GNP (21%), and CNF (2.2%). Meanwhile, a nano iron(II,III) oxide and nano nickel(II) oxide, major metal impurities in MWCNT, are also subjected to the SY electrochemical reaction, but failed to show any electrochemical current signals (Supporting Information Figure S2). The following conclusions may be drawn from the observation: (i) impure MWCNT is the best matrix for this electrochemical conversion, (ii) a chemical interaction between the oxygen-rich functional groups such as carbonyl and carboxylic acid of the f-MWCNT and amino functional groups of the intermediates is a likely reason for the large background current and the different qualitative electrochemical features with f-MWCNT modified electrode, (iii) graphite impurity in the impure-MWCNT is also responsible for the SY electrochemical oxidation reaction, (iv) although the metal oxide impurities in MWCNT did not influence the SY electrochemical oxidation, they might have helped to hold a large amount of the aniline intermediate species via metal-amino functional group complex, which in turn facilitates the SY electrochemical conversion, and (v) because the purified MWCNT sample contains fewer impurity levels, which might be less than the threshold limit, a feeble A3 peak current signal was observed.

On the basis of the overall results, possible electrochemical features of A1/C1-A4/C4 peaks are assigned as redox transitions of leucoemeraldine (A2/C2), emeraldine (A3/C3), and pernigraniline (A4/C4) forms of polyaniline.^{30,31} An irreversible peak observed in the first cycle of SY electrochemical reaction at 0.35 V vs Ag/AgCl is assigned as an azo bond electro-oxidation peak. Similarly, the A1/C1 redox peak noticed at -0.3 V vs Ag/AgCl is described as an electrochemical behavior of energetically different MWCNT-interacted leucoemeraldine molecule. In our previous work on anthraquinone (AQ) modified MWCNT system, we noticed similar kinds of prepeak corresponded to the energetically different MWCNT-AQ system.³² The observation of the highest A3/C3 redox response over the A1/C1 and A2/C2 redox peaks with GCE/MWCNT@SY-Oxid reveals a positive interaction between the MWCNT and emeraldine form of the polyaniline. A detailed physicochemical study is necessary to further understand the interaction.

Apart from the azo group, the phenolic functional group in SY may also be responsible for electrochemical reaction such as phenol oxidation to surface confined quinone product on the

MWCNT surface.²⁶ A continuous CV response of β -naphthol (control) adsorbed GCE/MWCNT in pH 7 PBS was carried out to find interference of the phenolic functional group of SY. As can be seen in Supporting Information Figure S3, a featureless voltammetric response was observed and indicates the absence of SY's phenolic group on the redox behavior of GCE/MWCNT@SY-CoPANI_{pH7}.

To understand the mechanistic aspect, the GCE/MWCNT@SY-CoPANI_{pH7} was subjected to various CV scan rates (10–300 mV s $^{-1}$) and pH's. A systematic increase in the peak current response (A3/C3) against increase in the scan rate was noticed (Figure 4A). A double logarithmic plot of scan rate

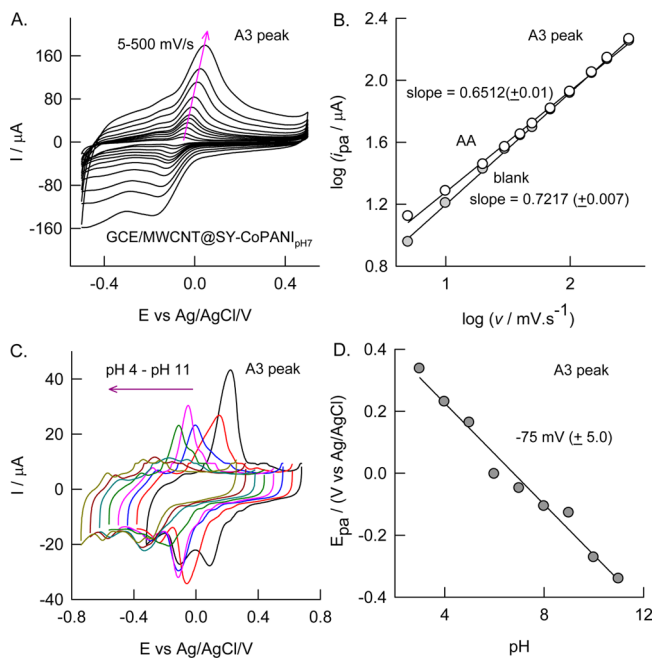


Figure 4. (A) Effect of scan rate (5–500 mV s $^{-1}$) on the CV of GCE/MWCNT@SY-CoPANI_{pH7} in pH 7 PBS. (B) Double logarithmic plot of anodic peak current (i_{pa}) vs scan rate. (C) Effect of solution pH (4–11) on the CV response of GCE/MWCNT@SY-CoPANI_{pH7} at a fixed scan rate of 50 mV s $^{-1}$. (D) Plot of E_{pa} (V vs Ag/AgCl) vs pH.

versus anodic peak current was linear with a slope value ($\partial \log i_{pa} / \partial \log v$) = 0.72, which is between the values of 0.5 and 1 for the diffusion and adsorption controlled electron-transfer systems, respectively, ascribed to the mixed adsorption and diffusion controlled electron-transfer feature of the redox peak (Figure 4B). Figure 4C is a CV of GCE/MWCNT@SY-CoPANI_{pH7} in varying pH solutions ranging from pH 3 to 10 at a scan rate = 50 mV s $^{-1}$. The peak potential of A3/C3 decreases regularly with increase of the solution pH. A plot of anodic peak potential, E_{pa} (A3), versus solution pH (Figure 4D) shows a linear line with a slope -75 ± 5 mV pH $^{-1}$ describing a non-Nernstian type mechanism with involvement of $3\text{H}^+/\text{2e}^-$ proton-coupled electron-transfer reaction.³³

3.2. Physico-chemical Characterizations of MWCNT@SY-CoPANI_{pH7}. Figure 5B and C shows TEM photographs of the GCE/MWCNT@SY-CoPANI_{pH7} layer taken under two different magnifications. Appearances of a blackish cloudy layer on net like CNTs at low magnifications and a bulged tube like structure at high magnification were noticed. A similar kind of observation was previously noticed in our preliminary study of electrochemical oxidation of aniline to surface confined

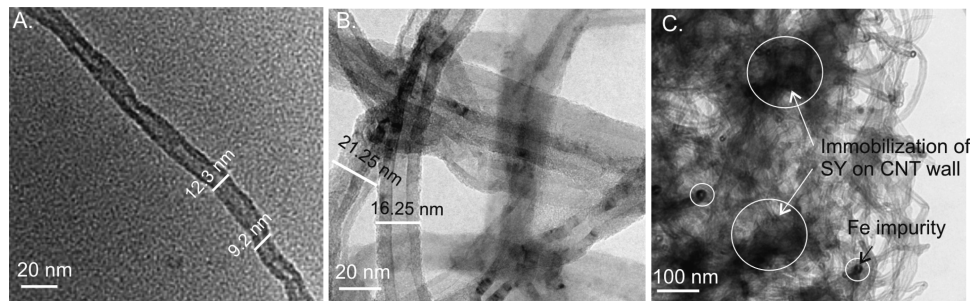


Figure 5. TEM images of (A) MWCNT (unmodified) and (B and C) MWCNT@SY-CoPANI_{pH7}.

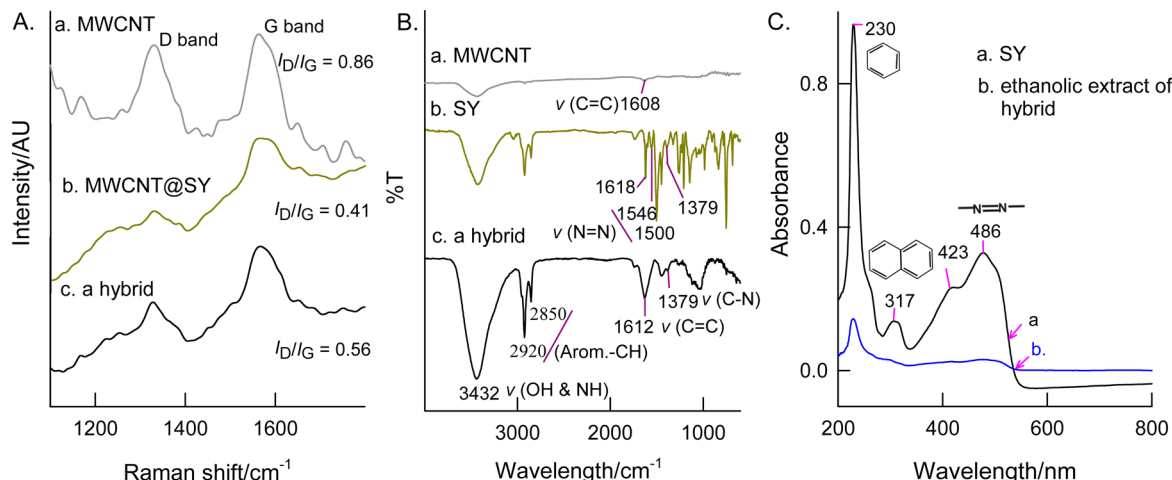


Figure 6. (A) Raman, (B) infrared, and (C) UV-visible spectroscopic responses of MWCNT@SY-CoPANI_{pH7} with its control systems.

polyaniline on GCE/MWCNT in a pH 7 PBS.³⁰ These TEM results provide first hand information about the existence of polymeric structure on the GCE/MWCNT@SY-CoPANI_{pH7}. Further, Raman spectroscopic characterization supports the result. Figure 6A, curves a–c, are the comparative Raman spectroscopic responses of MWCNT, MWCNT@SY, and MWCNT@SY-CoPANI_{pH7}. Specific peaks at frequencies 1570 and 1330 cm⁻¹, which correspond to the graphitic G and D bands, where the G and D bands are due to the pure graphite structure (sp^2 carbons) and disordered oxygen functionalities (sp^3 carbon units), respectively,³⁴ were noticed. The intensity ratio of the G and D bands, that is, I_D/I_G , can be taken as a measure of the graphitic structure versus oxygen functionalized graphitic units.³⁴ The ratio values, $I_D/I_G < 1$ and $I_D/I_G > 1$, can infer orderness and disorderness, respectively, of the graphitic units.³⁵ The calculated I_D/I_G values with pristine-MWCNT, MWCNT@SY, and MWCNT@SY-CoPANI_{pH7} were 0.86, 0.41, and 0.56, respectively. The higher I_D/I_G value observed with the MWCNT@SY-CoPANI_{pH7} (0.56) over the MWCNT@SY (0.41) supports the existence of polymeric aromatic structure with large sp^2 units on the MWCNT@SY-CoPANI_{pH7}. FTIR is a powerful tool to further identify specific functional groups in the MWCNT@SY-CoPANI_{pH7} system. As can be seen in Figure 6B, FTIR spectra of a naked SY (Figure 6B, curve b) showed specific stretching peaks at 3432, 1618, 1500–1546, and 1379 cm⁻¹ corresponding to vibrations of $-OH/-NH$, $-C=C-$, $-N=N-$, and C–N functional groups, respectively. Disappearance of the intense peak at 1500–1546 cm⁻¹ ($-N=N-$) and intensification of $-NH$ bond at 3432 cm⁻¹ clearly indicates the reductive cleavage of azo bond and formation of polymeric unit on MWCNT surface.

The SY and GCE/MWCNT@SY-CoPANI_{pH7} were further examined by UV-visible spectroscopy. An ethanolic extract of GCE/MWCNT@SY-CoPANI_{pH7}, prepared by sonication of the electrode in 500 μ L of ethanol, filtered using a microsyringe, was subjected to the analysis. Figure 6C, curves a and b, shows UV-vis patterns of SY and the ethanolic extract of MWCNT@SY-CoPANI_{pH7}, respectively. Note that the absorption peaks at 423 and 486 nm, which correspond to the azo linkage of SY³⁶ were diminished significantly after the electrochemical conversion of SY to SY-Oxid (SY-CoPANI_{pH7}) on the MWCNT surface. This result demonstrates the electrochemical decolorization and degradation of the azo dye. From the above physical and electrochemical characterizations results, it is concluded that the electrochemical reaction of SY on MWCNT follows reductive cleavage of azo bond at negative potential and subsequent oxidation to copolyaniline at positive potential of CV scan unusually in a neutral pH.

Like SY, some of the other azo dyes, Sudan red (SR) and methyl red (MR), were also subjected to a surface bound electrochemical reaction on MWCNT in pH 7 PBS (Supporting Information Figure S4). Interestingly, in all of these cases, different redox peak behaviors, which may be relating to decomposition of azo bond and formation of copolyaniline, are observed in MWCNT@SY-CoPANI_{pH7} and also depend upon the nature, ratio, and solubility of respective aniline intermediates.

3.3. Electroanalytical Features of GCE/MWCNT@SY-CoPANI_{pH7}. To examine the electroanalytical feature of the MWCNT@SY-CoPANI_{pH7}, AA oxidation and $Fe(CN)_6^{3-}$ redox reactions were studied as model systems. It is well-known that most of the carbon-based electrodes including

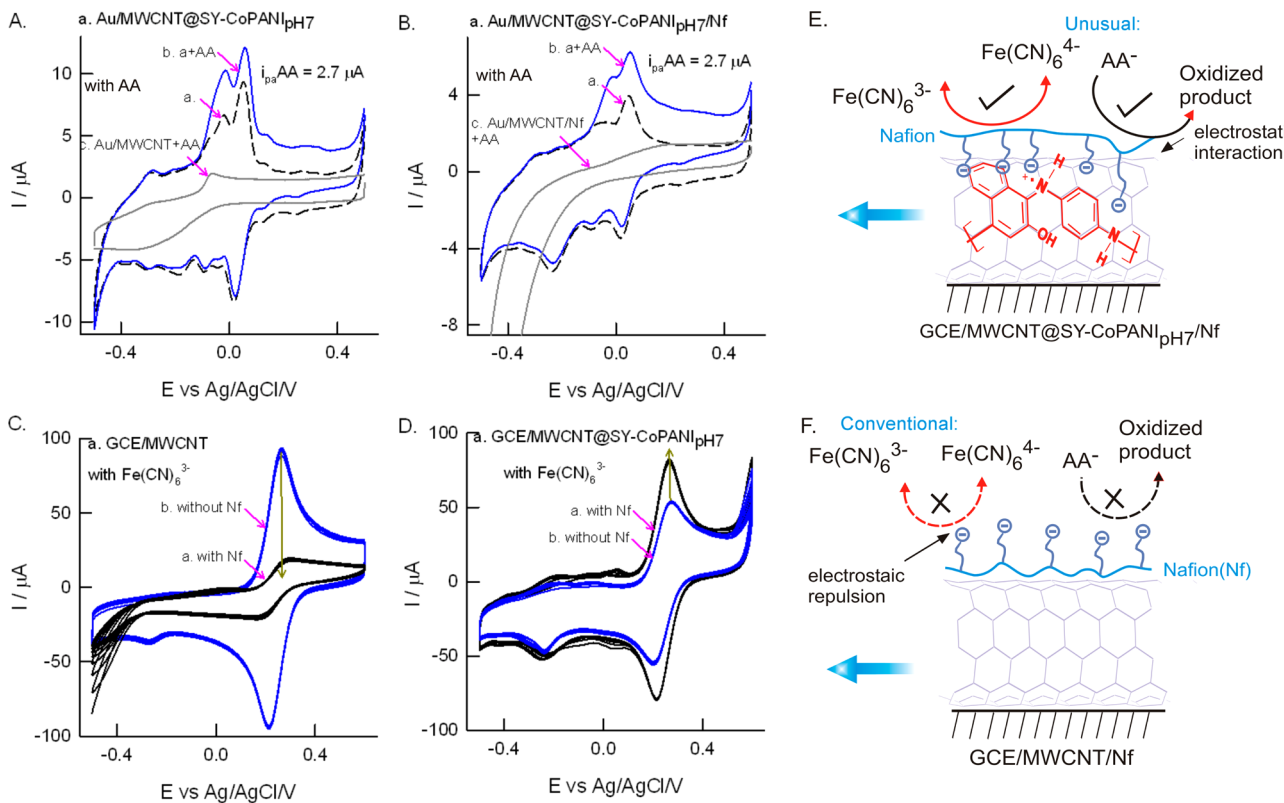


Figure 7. CV responses of Au or GCE/MWCNT (A and C) and Au or GCE/MWCNT@SY-CoPANI_{pH7} (B and D) and its respective Nafion coated systems, Au or GCE/MWCNT/Nf (A and C) and Au or GCE/MWCNT@SY-CoPANI_{pH7/Nf} (B and D) with 1 mM each ascorbic (A and B) acid and ferricyanide (C and D) at $v = 50 \text{ mV s}^{-1}$. For AA, pH 7 PBS was used, and for $\text{Fe}(\text{CN})_6^{3-}$, 0.1 M KCl was used as electrolyte. (E) and (F) are cartoons for the $\text{Fe}(\text{CN})_6^{3-}$ and AA electrochemical oxidation reactions on different modified electrodes.

GCE, MWCNT, graphite oxide, graphene, graphite, and polyaniline have appreciable electrocatalytic activity to AA oxidation; however, they suffer from surface fouling and high overpotential problems.^{37–39} Meanwhile, in some cases, to suppress the electrochemical behavior of AA, dilute Nafion solution, 0.5–1%, was generally coated on the working electrode, wherein the anionic form of AA (pK_a 4.10) was electrostatically repelled by the Nafion-sulfonic acid's ($-\text{SO}_3^-$) sites.⁴⁰ Thus, by studying the CV behavior of MWCNT@SY-CoPANI_{pH7} with the above models (AA and $\text{Fe}(\text{CN})_6^{3-}$) and Nafion, one can get information about the surface features easily (Figure 7). To avoid the influence of underlying carbon on the AA electro-oxidation reaction, a gold underlying substrate was taken to modify MWCNT@SY-CoPANI_{pH7}. The use of Au electrode as an electro-catalyst for AA oxidation reaction is not reported. Interestingly, Au/MWCNT@SY-CoPANI_{pH7} showed about 19, 7, and 9 times enhanced AA oxidation current signals than that of Au (data not enclosed), MWCNT, and Au/MWCNT/Nf systems, respectively (Figure 7A). After anionic Nafion film coating, no further alteration in the electro-oxidation signal of AA, besides a slight decrement in the redox feature of the modified electrode, was noticed (Figure 7B), which is different from the conventional methods that report with significantly suppressed AA oxidation current signals due to the electrostatic repulsion between the anionic form of AA and Nafion- SO_3^- (Scheme 1G and Figure 7E and F).⁴¹ This observation is quite unusual in the electrochemical sensing of AA in neutral pH. To further examine the surface feature, MWCNT@SY-CoPANI_{pH7} without or with Nf coating was subjected to $\text{Fe}(\text{CN})_6^{3-}$ experiment

as in Figure 7D. Interestingly, about 30 times higher redox behavior of the $\text{Fe}(\text{CN})_6^{3-/-4-}$ over the respective Nf unmodified electrode signal was noticed after the Nafion coating. The inactiveness of the Nafion-sulfonic acid in AA oxidation and the unusual acceleration of the $\text{Fe}(\text{CN})_6^{3-/-4-}$ redox reaction are probably due to the zwitter ionic interaction between the sulfonic acid and polaron like sites of copolymer of polyaniline and poly(1-amino-2-naphthol) (Scheme 1F).

Figure 8A and C shows typical calibration plots for sensing of AA by CV and amperometric $i-t$ (at 40 mV vs Ag/AgCl) methods in pH 7 PBS. Appreciable AA sensing behaviors were noticed. The CV current signal of AA at 500 μM –5 mM (Figure 8B) and amperometric $i-t$ current signal at 50–500 μM (Figure 8D) were found to be linear. The observed current sensitivity values were much higher than previously reported Nafion-based MWCNT and polyaniline electrochemical systems.^{42,43} In continuation, a flow injection analysis of AA using a GCE/MWCNT@SY-CoPANI_{pH7/Nf}, as a detector, was also demonstrated. FIA signals of AA were linear in a concentration window 10–5000 μM at applied potential, 40 mV vs Ag/AgCl, and hydrodynamic flow rate, 0.7 mL min⁻¹ (Figure 9A). The calculated AA detection limit values by amperometric $i-t$ and FIA are 18.3 and 24.5 μM , respectively. Except cysteine, no other electro-active chemicals such as uric acid (UA), glucose (Glu), citric acid (CA), nitrite (NO_2^-), and nitrate (NO_3^-) interfered with the sensing of AA (Figure 9B). Further, to validate the analytical protocol of the present sensor, FIA of AA in a fruit juice (#1) (Figure 9C) and four different real samples (Supporting Information Figure S6, #2–#5) were examined by standard addition approach, and the

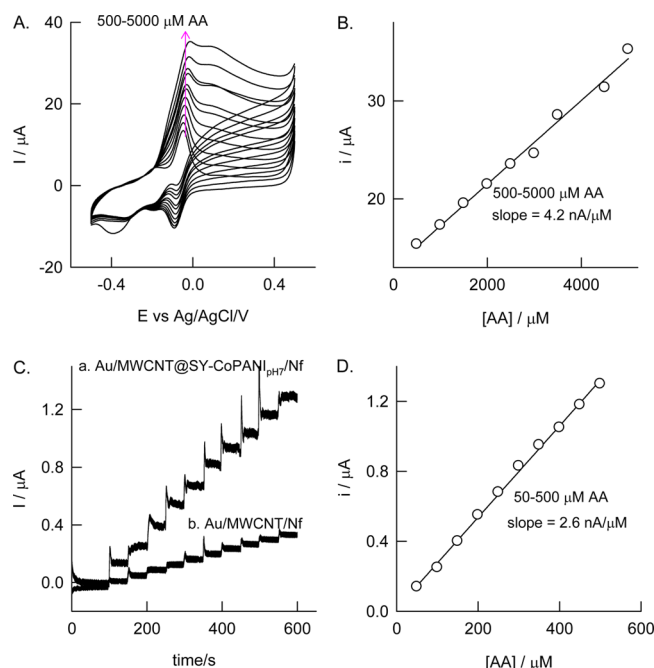


Figure 8. (A) Effect of AA concentration on the CV of GCE/MWCNT@SY-CoPANI_{pH7} modified electrode in pH 7 PBS at scan rate of 10 mV s⁻¹. (C) Comparative amperometric *i*-*t* responses of Au/MWCNT@SY-CoPANI_{pH7}/Nf (a) and Au/MWCNT/Nf (b) for continuous spikes of 50 μM AA at an applied potential of 40 mV vs Ag/AgCl and (B and D) respective plots of [AA] versus current.

results obtained were quite satisfactory with the good recovery values (Supporting Information Table S1).

4. CONCLUSIONS

Sudan yellow azo dye gets electro-reduced into aniline and 1-amino-2-naphthol intermediates and further electro-oxidized into copolymer of polyaniline and poly(1-amino-2-naphthol) on a MWCNT surface unusually in a neutral pH solution. Control cyclic voltammetric experiments with aniline and 1-amino-2-naphthol supported the observation. The new chemically modified electrode (MWCNT@CoPANI_{pH7}) showed highly stable redox signals upon continuous CV cycling in pH 7 phosphate buffer solution. The in situ CV-EQCM experiment confirmed the formation of aniline as one of the intermediates during the SY electrochemical reaction on MWCNT. Collective

physicochemical characterization using TEM, Raman, IR, and UV spectroscopic techniques further confirmed the formation of copolymer of polyaniline and poly(1-amino-2-naphthol) via electrochemical oxidation of aniline and 1-amino-2-naphthol intermediate on the MWCNT surface. No such polymer formation was observed when MWCNT was replaced by a conventional electrode like GCE. The MWCNT@SY-CoPANI_{pH7} showed about 7–19 times higher electrocatalytic oxidation signal of AA over the GCE and MWCNT in a neutral pH solution. The electrocatalytic activity of AA on the modified electrode with Nafion was found to be significantly higher than that of the conventional Nafion-based electrodes, which suffered from suppressed electrochemical activity due to the electrostatic repulsion between the anionic functional groups of AA and Nafion. This newly developed analytical method is further validated by detecting the AA concentration in various real samples with recovery values ~100%.

■ ASSOCIATED CONTENT

● Supporting Information

Detailed experimental procedures, control CV responses of Sudan yellow dye modified on GCE/Fe₂O₃ and GCE/NiO, CV responses of β-naphthol, methyl red, and Sudan red dyes on GCE/MWCNT, effect of applied potential on the CV of GCE/MWCNT@SY in pH 7 PBS, optimization of FIA's flow rate for AA using GCE/MWCNT@SY-CoPANI_{pH7}/Nf detector, FIA of ascorbic in three real samples (pharmaceutical tablets and food supplement samples), and its relevant analytical data. This material is available free of charge via the Internet at <http://pubs.acs.org>.

■ AUTHOR INFORMATION

Corresponding Author

*Phone: +91-416-2202754. E-mail: askumarchem@yahoo.com.

Notes

The authors declare no competing financial interest.

■ ACKNOWLEDGMENTS

We gratefully acknowledge the Department of Science and Technology-Science and Engineering Research Council Scheme (DST-SERC) for the financial support. We also thank DST-Technology System Development (DST-TSD) for the FIA-ECD.

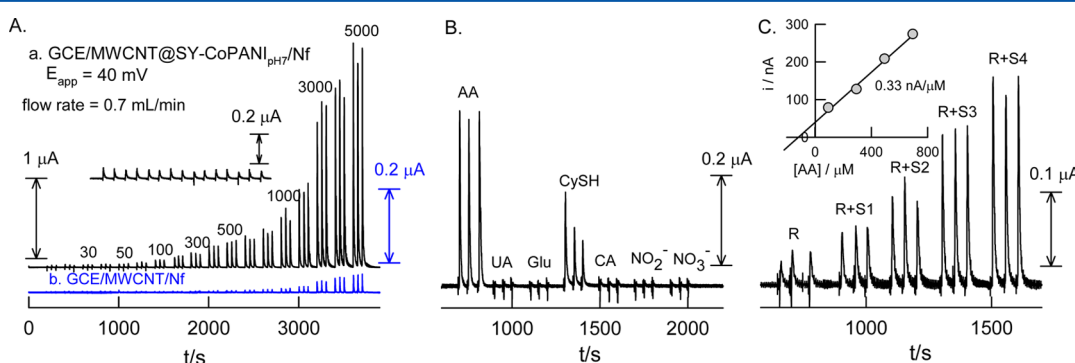


Figure 9. FIA responses of (A) GCE/MWCNT@SY-CoPANI_{pH7}/Nf (a) and GCE/MWCNT/Nf with different concentrations of AA, (B) GCE/MWCNT@SY-CoPANI_{pH7}/Nf with different interfering chemicals, and (C) typical detection of AA in a grape juice real sample (#1). E_{app} = 40 mV versus Ag/AgCl and flow rate = 0.7 mL min⁻¹ in pH 7 PBS. UA = uric acid, Glu = glucose, CySH = cysteine, CA = citric acid, NO₂⁻ = nitrite, and NO₃⁻ = nitrate.

REFERENCES

- (1) Chudgar, R. J.; Oakes, J. Dyes, Azo. In *Encyclopedia of Chemical Technology*; Othmer, K., Ed.; John Wiley & Sons, Inc.: New York, 2001.
- (2) Aspland, J. R. *Textile Dyeing and Coloration*; American Association of Textile Chemists and Colorists: NC, 1997.
- (3) Golka, K.; Kopp, S.; Myslak, Z. W. Carcinogenicity of Azo Colorants: Influence of Solubility and Bioavailability. *Toxicol. Lett.* **2004**, *151*, 203–210.
- (4) Stiborova, M.; Martinek, V.; Rydlova, H.; Hodek, P.; Frei, E. Sudan I is a Potential Carcinogen for Humans: Evidence for its Metabolic Activation and Detoxification by Human Recombinant Cytochrome p450 1A1 and Liver Microsomes. *Cancer Res.* **2002**, *62*, 5678–5684.
- (5) Gordon, J. Contact Reactivity to Azo Dye Carcinogens. *Nature* **1964**, *203*, 884–885.
- (6) Chung, K.-T.; Stevens, S. E.; Cerniglia, C. E. The Reduction of Azo Dyes by the Intestinal Microflora. *Crit. Rev. Microbiol.* **1992**, *18*, 175–190.
- (7) Puntener, A.; Page, C. European Ban on Certain Azo Dyes – A Report. Quality and Environment, TFL, 2007.
- (8) Pinheiro, H. M.; Touraud, E.; Thomas, O. Aromatic Amines from Azo Dye Reduction: Status Review with Emphasis on Direct UV Spectrophotometric Detection in Textile Industry Wastewaters. *Dyes Pigm.* **2004**, *61*, 121–139.
- (9) Aleboyeh, A.; Olya, M. E.; Aleboyeh, H. Oxidative Treatment of Azo dyes in Aqueous Solution by Potassium Permanganate. *J. Hazard. Mater.* **2009**, *162*, 1530–1535.
- (10) Yu, H.; Chen, S.; Quan, X.; Zhao, H.; Zhang, Y. Fabrication of a TiO₂-BDD Heterojunction and its Application As a Photocatalyst for the Simultaneous Oxidation of an Azo Dye and Reduction of Cr(VI). *Environ. Sci. Technol.* **2008**, *42*, 3791–3796.
- (11) Ertugay, N.; Acar, F. N. Color and COD Removal of Azo Dye “Basic Blue 9” by Fenton Oxidation Process: Determined of Optimal Parameters and Kinetic Study. *J. Adv. Oxid. Technol.* **2013**, *16*, 268–274.
- (12) Konstantinou, I. K.; Albanis, T. A. TiO₂-Assisted Photocatalytic Degradation of Azo Dyes in Aqueous Solution: Kinetic and Mechanistic Investigations A review. *Appl. Catal., B* **2004**, *49*, 1–14.
- (13) Szpyrkowicz, L.; Radaelli, M.; Daniele, S. Electrocatalysis of Chlorine Evolution on Different Materials and Its Influence on the Performance of an Electrochemical Reactor for Indirect Oxidation of Pollutants. *Catal. Today* **2005**, *100*, 425–429.
- (14) Zhou, M.; Yu, Q.; Lei, L.; Barton, G. Electro-Fenton Method for the Removal of Methyl Red in an Efficient Electrochemical System. *Sep. Purif. Technol.* **2007**, *57*, 380–387.
- (15) Brown, D.; Humberger, B. The Degradation of Dyestuffs. III. Investigations of their Ultimate Biodegradability. *Chemosphere* **1987**, *16*, 1539–1553.
- (16) Pandey, A.; Singh, P.; Iyengar, L. Bacterial Decolorization and Degradation of Azo Dyes. *Int. Biodeterior. Biodegrad.* **2007**, *59*, 73–84.
- (17) Pumera, M. The Electrochemistry of Carbon Nanotubes: Fundamentals and Applications. *Chem.—Eur. J.* **2009**, *15*, 4970–4978.
- (18) Sang, Y.; Wang, B.; Wang, Q.; Zhao, G.; Guo, P. Insights into the Electrocatalysis of Nitrobenzene using Chemically-Modified Carbon Nanotube Electrodes. *Sci. Rep.* **2014**, *4*, 1–6.
- (19) Bia, H.; Li, Y.; Liu, S.; Guo, P.; Wei, Z.; Lv, C.; Zhang, J.; Zhao, X. S. Carbon-Nanotube-Modified Glassy Carbon Electrode for Simultaneous Determination of Dopamine, Ascorbic Acid and Uric Acid: The Effect of Functional Groups. *Sens. Actuators, B* **2012**, *171–172*, 1132–1140.
- (20) Machado, F. M.; Bergmann, C. P.; Fernandes, T. H. M.; Lima, E. C.; Royer, B.; Calvete, T.; Fagan, S. B. Adsorption of Reactive red M-2BE Dye from water Solutions by Multi-walled Carbon Nanotubes and Activated Carbon. *J. Hazard. Mater.* **2011**, *192*, 1122–1131.
- (21) Khataee, A. R.; Safarpour, M.; Zarei, M.; Aber, S. Combined Heterogeneous and Homogeneous Photodegradation of a Dye using Immobilized TiO₂ Nanophotocatalyst and Modified Graphite Electrode with Carbon Nanotubes. *J. Mol. Catal. A: Chem.* **2012**, *363*, 58–68.
- (22) Kumar, A. S.; Gayathri, P. Organic Redox Mediators Functionalized CNT Chemically-Modified Electrodes for Electrochemical Applications. In *Handbook of Functional Nanomaterials*; Aliofkhazraei, M., Ed.; Nova Science Publishers Inc.: US, 2013; pp 377–392.
- (23) Genies, E. M.; Pennem, J. F.; Lapkowski, M. Polyanilines from Electropolymerization of Azobenzene. *J. Electroanal. Chem.* **1989**, *260*, 145–156.
- (24) Kumar, A. S.; Gayathri, P.; Barathi, P.; Vijayaraghavan, R. Improved Electric Wiring of Hemoglobin with Impure-Multiwalled Carbon Nanotube/Nafion Modified Glassy Carbon Electrode and Its Highly Selective Hydrogen Peroxide Biosensing. *J. Phys. Chem. C* **2012**, *116*, 23692–23703.
- (25) Xie, Q.; Li, Z.; Deng, C.; Liu, M.; Zhang, Y.; Ma, M.; Xia, S.; Xiao, X.; Yin, D.; Yao, S. Electrochemical Quartz Crystal Microbalance Monitoring of the Cyclic Voltammetric Deposition of Polyaniline. *J. Chem. Educ.* **2007**, *84*, 681–684.
- (26) Sornambikai, S.; Kumar, A. S. Selective Immobilization of Hydroquinone on Carbon Nanotube Modified Electrode via Phenol Electro-oxidation Method and its Hydrazine Electro-catalysis and Escherichia coli Antibacterial Activity. *Electrochim. Acta* **2012**, *62*, 207–217.
- (27) Swetha, P.; Shalini devi, K. S.; Kumar, A. S. In-situ Trapping and Confining of Highly Redox Active Quinolone Quinones on MWCNT Modified Glassy Carbon Electrode and its Selective Electrocatalytic Oxidation and Sensing of Hydrazine. *Electrochim. Acta* **2014**, *147*, 62–72.
- (28) Barathi, P.; Kumar, A. S. Facile Electrochemical Oxidation of Polyaromatic Hydrocarbons to Surface-Confined Redox-Active Quinone Species on a Multiwalled Carbon Nanotube Surface. *Chem.—Eur. J.* **2013**, *19*, 2236–2241.
- (29) Barathi, P.; Kumar, A. S. Electrochemical Conversion of Unreactive Pyrene to Highly Redox-Active 1,2-quinone Derivatives on a Carbon Nanotube-Modified Gold Electrode Surface and its Selective Hydrogen Peroxide Sensing. *Langmuir* **2013**, *29*, 10617–10623.
- (30) Vishnu, N.; Kumar, A. S.; Pillai, K. C. Unusual Neutral pH Assisted Electrochemical Polymerization of Aniline on a MWCNT Modified Electrode and its Enhanced Electro-Analytical Features. *Analyst* **2013**, *138*, 6296–6300.
- (31) Dennany, L.; Innis, P. C.; McGovern, S. T.; Wallace, G. G.; Forster, R. J. Electronic Interactions within Composites of Polyanilines Formed Under Acidic and Alkaline Conditions. Conductivity, ESR, Raman, UV-Vis and Fluorescence Studies. *Phys. Chem. Chem. Phys.* **2011**, *13*, 3303–3310.
- (32) Kumar, A. S.; Swetha, P. Simple Adsorption of Anthraquinone on Carbon Nanotube Modified Electrode and its Efficient Electrochemical Behaviors. *Colloids Surf., A* **2011**, *384*, 597–604.
- (33) Mandic, Z.; Nigovic, B.; Simuni, B. The Mechanism and Kinetics of the Electrochemical Cleavage of Azo Bond of 2-Hydroxy-5-Sulfophenyl-Azo-Benzoic Acids. *Electrochim. Acta* **2004**, *49*, 607–615.
- (34) McCreery, R. L. Advanced Carbon Electrode Materials for Molecular Electrochemistry. *Chem. Rev.* **2008**, *108*, 2646–2687.
- (35) Holloway, A. F.; Wildgoose, G. G.; Compton, R. G.; Shao, L.; Green, M. L. H. The Influence of Edge-Plane Defects and Oxygen-Containing Surface Groups on the Voltammetry of Acid-Treated, Annealed and “Super-Annealed” Multiwalled Carbon Nanotubes. *J. Solid State Electrochem* **2008**, *12*, 1337–1348.
- (36) Styliadi, M.; Kondarides, D. I.; Verykios, X. E. Pathways of Solar Light-Induced Photocatalytic Degradation of Azo Dyes in Aqueous TiO₂ Suspensions. *Appl. Catal., B* **2003**, *40*, 271–286.
- (37) Zhang, L.; Jiang, X. Attachment of Gold Nanoparticles to Glassy Carbon Electrode and its Application for the Voltammetric Resolution of Ascorbic Acid and Dopamine. *J. Electroanal. Chem.* **2005**, *583*, 292–299.
- (38) Noroozifar, M.; Khorasani-Motlagh, M.; Tavakkoli, H. Preparation of Tetraheptylammonium Iodide-Iodine Graphite-Multiwall Carbon Nanotube Paste Electrode: Electrocatalytic Determination of Ascorbic Acid. *J. Phys. Chem. C* **2013**, *117*, 1337–1344.

nation of Ascorbic Acid in Pharmaceuticals and Foods. *Anal. Sci.* **2011**, *27*, 929–935.

(39) Ghica, M. E.; Wintersteller, Y.; Brett, C. M. A. Poly(brilliant green)/Carbon nanotube-Modified Carbon Film Electrodes and Application as Sensors. *J. Solid State Electrochem.* **2013**, *17*, 1571–1580.

(40) Ali, S. R.; Ma, Y.; Parajuli, R. R.; Balogun, Y.; Lai, W. Y.-C.; He, H. A Nonoxidative Sensor Based on a Self-Doped Polyaniline/Carbon Nanotube Composite for Sensitive and Selective Detection of the Neurotransmitter Dopamine. *Anal. Chem.* **2007**, *79*, 2583–2587.

(41) Tiwari, I.; Singh, K. P.; Singh, M.; Banks, C. E. Polyaniline/Polyacrylic Acid/Multi-Walled Carbon Nanotube Modified Electrodes for Sensing Ascorbic acid. *Anal. Methods* **2012**, *4*, 118–124.

(42) Liu, M.; Wen, Y.; Li, D.; Yue, R.; Xu, J.; He, H. A Stable Sandwich-Type Amperometric Biosensor Based on Poly(3,4-ethylenedioxythiophene)-Single Walled Carbon Nanotubes/Ascorbate Oxidase/Nafion Films for Detection of L-Ascorbic Acid. *Sens. Actuators, B* **2011**, *159*, 277–285.

(43) Liu, M.; Wen, Y.; Xu, J.; He, H.; Li, D.; Yue, R.; Liu, G. An Amperometric Biosensor Based on Ascorbate Oxidase Immobilized in Poly(3,4-ethylenedioxythiophene)/Multi-Walled Carbon Nanotubes Composite Films for the Determination of L-Ascorbic Acid. *Anal. Sci.* **2011**, *27*, 477–482.